EFFECTS OF HYDROGEN CHARGE ON CYCLIC STRESS-STRAIN PROPERTIES AND FATIGUE BEHAVIOUR

Hideyuki UYAMA*, Yoji MINE**, Yukitaka MURAKAMI**
*NSK Ltd. Currently at Graduate School of Engineering, Kyushu University,
Hakozaki, Higashi-ku, Fukuoka 812-8581, Japan
** Department of Mechanical Engineering Science, Kyushu University,
Hakozaki, Higashi-ku, Fukuoka 812-8581, Japan
e-mail: mine@mech.kyushu-u.ac.jp

Abstract

Effects of hydrogen charge on fatigue behaviour of carbon steels were investigated. In the 0.13% C steel hydrogen charge did not affect the stress-strain hysteresis loops; on the other hand, in the 0.47% C steel the strain amplitude was decreased by hydrogen charge. From the results of the constant stress amplitude tests of the 0.47% C steel, a difference in the strain amplitude profile and the saturation value was obtained between the hydrogen-charged and uncharged specimens. These imply that effects of hydrogen charge on cyclic stress-strain properties vary with material and/or hydrogen content. The effect of hydrogen charge on the fatigue life was not remarkable, while there is a distinct difference in the appearance of the slip bands between the hydrogen-charged and uncharged specimens. The localisation of slip bands was observed in the hydrogen-charged specimen. Therefore, the decrease in the strain amplitude by hydrogen charge is deduced to be caused by the localised slip bands.

Introduction

It is known that the fatigue failure, which occurs at stresses lower than the conventional fatigue limit, arises from internal fracture. Murakami *et al* pointed out that an optically dark area, which is referred to ODA, beside inclusion is observed on the ultralong fatigue fracture surfaces of high strength steels [1, 2]. According to their observation it is presumed that the mechanism forming the ODA is related to hydrogen trapped by the inclusion at fracture origin [3, 4]. It is crucially important to understand the role of hydrogen on fatigue behaviour in order to clarify the mechanism forming the ODA. Recent progress of development of fuel cell (FC) systems and hydrogen combustion engines requires the safety assessment of the metallic materials used in these systems from the view point of hydrogen degradation. Although it has been reported that hydrogen degrades mechanical properties of metallic materials [5, 6], there have been few studies on the effect of hydrogen on fatigue behaviour. In the present study, the fatigue behaviour of carbon steels was studied to understand fundamental phenomena of metal fatigue in hydrogen environments.

Experimental Procedure

The materials used in this study were round bars made of a 0.13% carbon steel and a 0.47% carbon steel. The round bars of the 0.13% C and 0.47% C steels were 22 mm and 25 mm in diameter, respectively. Table 1 shows the chemical compositions of the materials. The round bars of the 0.13% C and 0.47% C steels were heated to temperatures of 1173 K and 1117 K, respectively, and held for 1 hour, and then furnace cooled to room temperature. Subsequently, the round bars were machined to fatigue specimens. In the longitudinal directions, both annealed round bars had the banded microstructures which had been formed in the rolling process. Figures 1 (a) and (b) show the microstructures, which consist of ferrite

(bright area) and pearlite (dark area) ones, of the annealed 0.13% C and 0.47% C steels, respectively. The hardness of the annealed 0.13% C and 0.47% C steels was $H_v = 105$ and 170, respectively.

TABLE 1. Chemical compositions of materials.

(mass %)

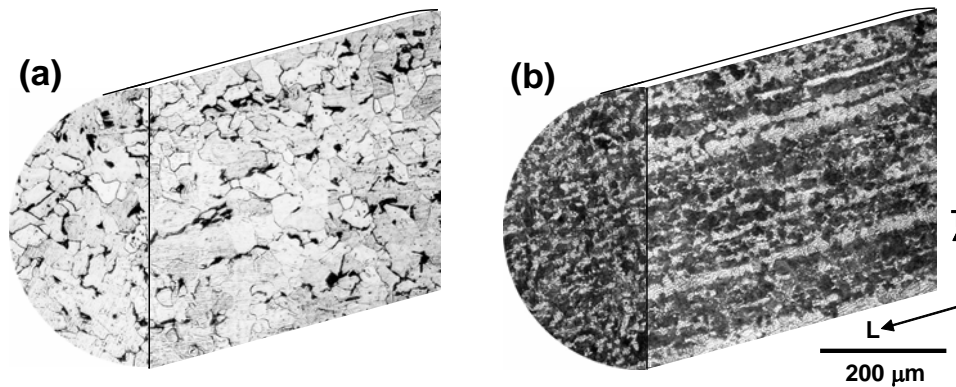|	C	Si	Mn	P	S	Cu	Al	Ni+Cr	Fe
0.13% C steel	0.13	0.22	0.39	0.013	0.022	0.09	0.01	0.10	Bal.
0.47% C steel	0.47	0.19	0.70	0.012	0.024	-	0.024	0.12 (Cr)	Bal.

FIGURE 1. Microstructures of (a) 0.13% C steel and (b) 0.47% C steel.

Figures 2 (a) and (b) show plain and shallow-notched tension-compression fatigue specimens, respectively. The introduction of shallow notch into the specimen facilitated to observe the nucleation of slip bands and cracks because their nucleation sites were restricted in the notch root. The specimen surface for the measurement of cyclic stress-strain response was polished with emery paper #500. The specimen surface for S-N data was polished with emery paper #2000 and was finished by using polishing powder of 7 μm in diameter. The root of the shallow notch was finished with polishing powder of 0.3 μm in diameter. The hydrogen-charged and pre-fatigued specimens were re-polished immediately before fatigue tests in order to eliminate the flaws formed by hydrogen charge and pre-fatigue. Charging hydrogen into specimens was performed by immersing them in an aqueous solution of 20 mass% NH$_4$SCN at 310K for 24 hours. The hydrogen content in the specimen was measured by the thermal desorption spectrometry (TDS) within 2 hours after hydrogen charge. Although the TDS specimen was different from the fatigue specimen, the condition of the hydrogen charge was similar in both cases. Fatigue tests were carried out at room temperature in laboratory air. All the fatigue tests were conducted at a stress ratio, $R = -1$, by tension-compression. To obtain stress-strain hysteresis loops, load-controlled tests were performed at a frequency of 1 Hz and the strain responses were measured by an extensometer. The fatigue tests for S-N data were conducted at a frequency of 20 Hz. The

nucleation of slip bands and cracks was observed by a replica method in the shallow-notched specimen (stress concentration factor, K_t = 1.42) shown in Fig. 2 (b).

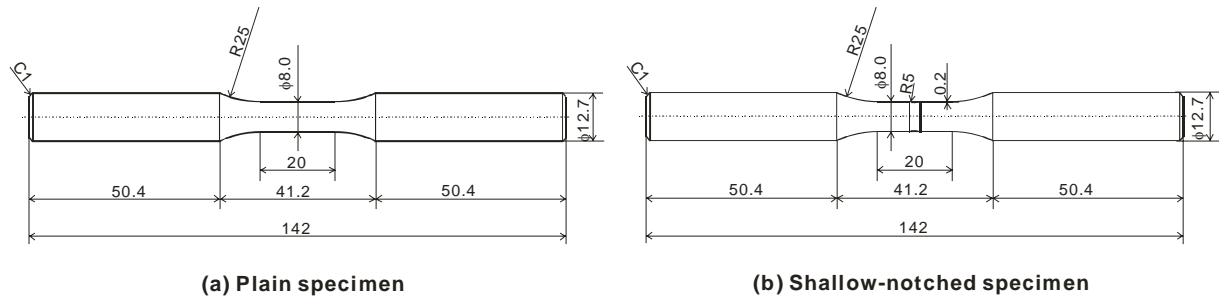**(a) Plain specimen**   **(b) Shallow-notched specimen**

FIGURE 2. Tension-compression fatigue specimens.

Experimental Results and Discussion

Change of Hydrogen Content

The hydrogen contents, which varied with the combination of pre-fatigue and hydrogen charge, of the 0.13% C and 0.47% C steels are summarised in Table 2. An about ten-fold increase in the hydrogen content was achieved by hydrogen charge for 24 hours without pre-fatigue. Hydrogen charge after pre-fatigue resulted in an increase in hydrogen absorption. The pre-fatigue was conducted at σ = 260 MPa, R = -1, f = 1 Hz and $N \approx 700$. The hydrogen contents of the 0.47% C steel were higher than those of the 0.13% steel in each case.

TABLE 2. Hydrogen Contents of materials.

(mass ppm)

Material	H-uncharged	H-charged	Pre-fatigued + H-charged
0.13% C steel	0.02	0.18	0.24
0.47% C steel	0.05	0.52	0.84

Effects of Hydrogen Charge on Cyclic Stress-Strain Properties

Figures 3 (a) and (b) show the comparisons of stress-strain hysteresis loops between the hydrogen-charged and uncharged specimens of the 0.13% C and 0.47% C steels, respectively. These hysteresis loops were measured with stress amplitude increased every 100 cycles, and were not much different from the hysteresis loops obtained with stress amplitude decreased in a similar way. The specimens of the 0.13% C and 0.47% C steels were hydrogen-charged after pre-fatigued at σ = 260 MPa and 300 MPa, respectively, and R = -1, f = 1 Hz and N = 300. Taking account of effects of strain aging, the hydrogen-uncharged specimen was left at room temperature for the same time that the hydrogen charge was performed before the hysteresis loop measurement. In the 0.13% C steel there was no difference in the hysteresis loops between the hydrogen-charged and uncharged specimens, while in the 0.47% C steel strain amplitude responses for stress amplitudes were smaller in the hydrogen-charged specimen than in the hydrogen-uncharged specimen. These results indicate effects of

hydrogen charge on cyclic stress-strain properties vary with material and/or hydrogen content.

Figure 4 shows the total strain amplitude responses of the hydrogen-charged and uncharged specimens without pre-fatigue for constant stress amplitude tests. In the hydrogen-uncharged specimen of the 0.13% C steel, the total strain amplitude was approximately 0.002 when the fatigue test started. Cyclic stressing of more than 200 cycles abruptly increased the total strain amplitude to the peak, and then the total strain amplitude was gradually decreased to 0.0037 in 1500 cycles. This rapid increase in the strain amplitude of the hydrogen-uncharged specimen is presumed to correspond to the so-called yield point phenomenon. Plastic deformation starts in a grain with appropriate crystallographic orientation to form slip bands and then spreads to the neighbouring grains one after another. This leads to the rapid increase in the strain amplitude of the hydrogen-uncharged specimen. On the other hand, the total strain amplitude of the hydrogen-charged specimen slowly increased, and in about 1200 cycles became equivalent to that of the hydrogen-uncharged specimen. The hydrogen-uncharged specimen of the 0.47% C steel was similar in the total strain amplitude profile to that of the 0.13% C steel. Although the total strain amplitude of the hydrogen-charged specimen of the 0.47% C steel gradually increased with increasing number of cycles, the saturation value of the hydrogen-charged specimen did not reach that of the hydrogen-uncharged specimen.
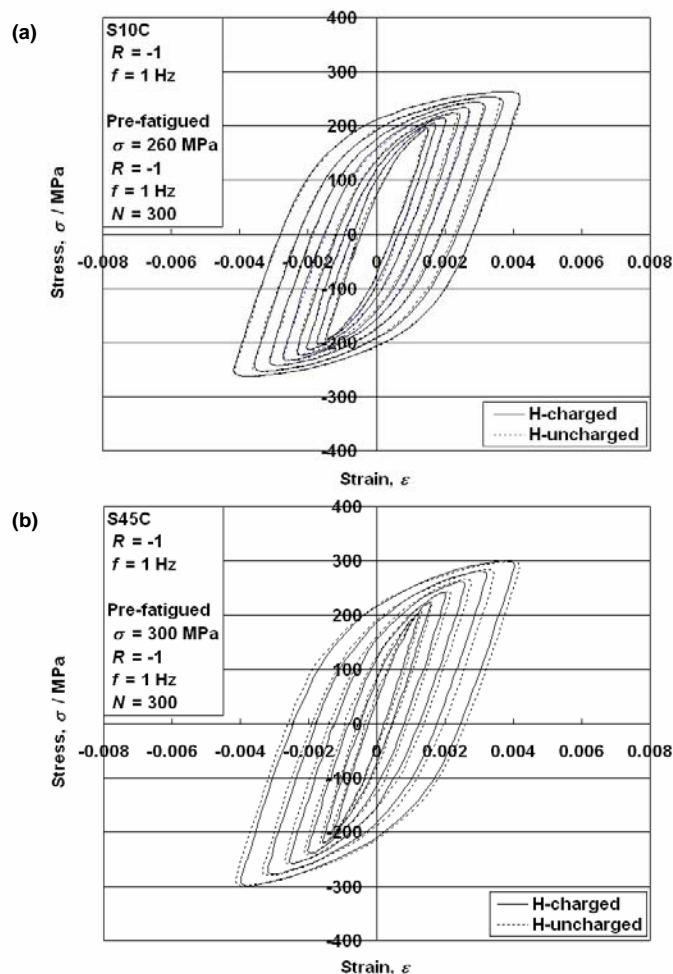

FIGURE 3. Stress-strain hysteresis loops of the hydrogen-charged and uncharged specimens of (a) 0.13% C steel and (b) 0.47% C steel.
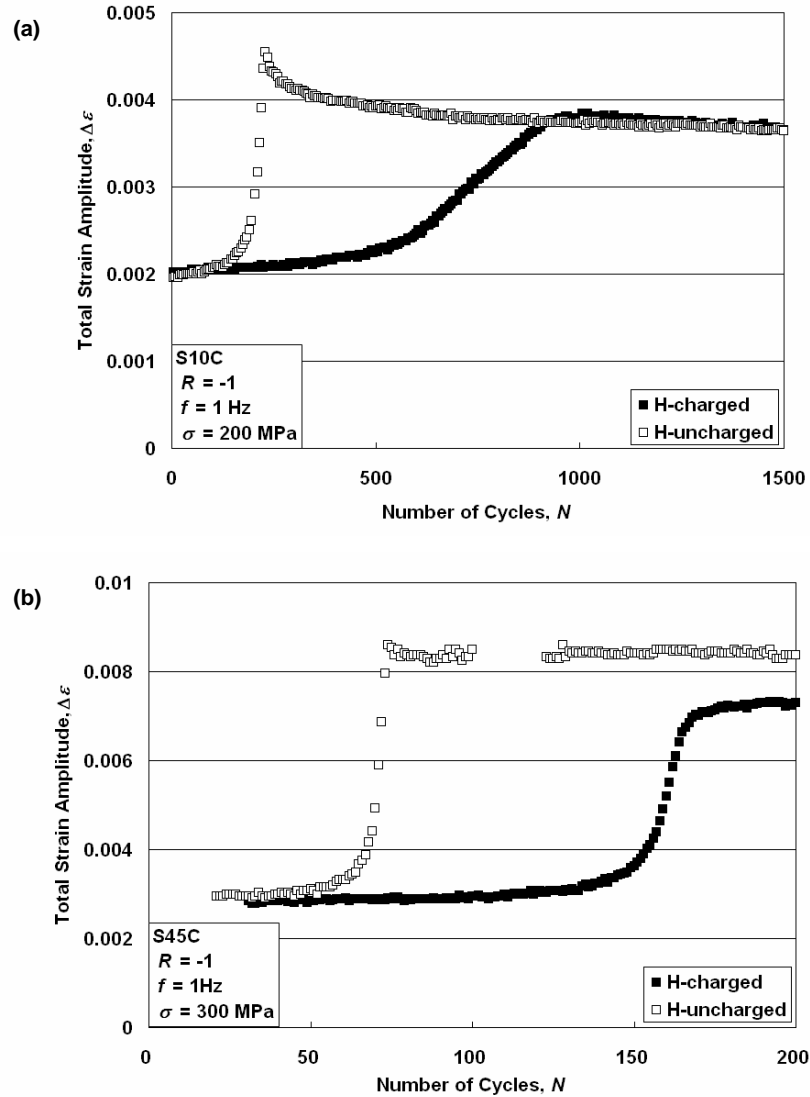
FIGURE 4. Total strain amplitude responses of the hydrogen-charged and uncharged specimens of (a) 0.13% C steel and (b) 0.47% C steel for constant stress amplitude tests.

These cyclic stress-strain data imply that although the effect introduced by hydrogen charge is maintained during the cyclic stressing in the 0.47% C steel, the effect diminishes in the early stage of the cyclic stressing in the 0.13% C steel. The hydrogen charge provided an increase of an order of magnitude in hydrogen content as listed in Table 2. The hydrogen content was further increased by hydrogen charge after pre-fatigue. This is caused by an increase in the glissile dislocation which effectively acts as a trapping site for hydrogen. The hydrogen contents were higher in the 0.47% C steel than in the 0.13% C steel in each case. The 0.47% C steel includes more pearlite microstructure, which is considered to serve to trap hydrogen effectively [7], compared to the 0.13% C steel. Therefore, in the 0.47% C steel with much pearlite microstructure, it is suggested that the pearlite microstructure serves as a supplier of hydrogen during cyclic stressing. Thus, the effects of hydrogen on cyclic stress-strain properties are maintained. On the other hand, in the 0.13% C steel containing ferrite microstructure mainly, if the hydrogen content is increased by the introduction of glissile dislocations, cyclic stressing during fatigue tests allows the glissile dislocations to act and leads to emission of hydrogen or hydrogen-trapping into the sites in which hydrogen does not affect dislocations.

Effects of Hydrogen Charge on Fatigue Behaviour

Figure 5 compares the *S-N* data for the hydrogen-charged specimens with that for the hydrogen-uncharged specimens in the 0.47% C steel. No significant difference in the *S-N* data was observed between the hydrogen-charged and uncharged specimens without pre-fatigue, even though hydrogen charge brought about an increase in the hydrogen content by about an order of magnitude and a decrease in the strain amplitude for the constant stress amplitude tests.

To study influences of hydrogen on microscopic behaviour, nucleation of slip bands and, initiation and propagation of cracks were observed in the shallow-notched specimens of the 0.47% C steel. Figure 6 represents the optical micrographs showing the processes of slip band nucleation, crack initiation and propagation in the hydrogen charged and uncharged specimens without pre-fatigue. Fatigue lives of the hydrogen-charged and uncharged specimens at $\sigma = 230$ MPa were $N_f = 2.16$ x 10^5 and 2.53 x 10^5, respectively. Although the fatigue lives are similar, there was a definite difference in the appearances of slip bands between the hydrogen-charged and uncharged specimens as shown in Fig.6. In the hydrogen-uncharged specimen the slip bands densely occurred every grain, and were widely distributed. In the hydrogen-charged specimen the slip bands were sparsely formed and localised. In both specimens cracks were initiated along concentrated slip bands and grew to link the slip bands. We re-experimented at $\sigma = 229$ MPa because the detailed observation in progress was not conducted in the experiment shown in Fig. 6. The appearance of slip bands was the same as shown in Fig. 6 However, contrary to the result shown in Fig. 6, the fatigue life ($N_f = 3.15$ x 10^5) of the hydrogen-charged specimen was longer than that ($N_f = 2.38$ x 10^5) of the hydrogen-uncharged specimen. Figure 7 shows the relationship between the surface crack length, $2a$ and the dimensionless number of cycles, N/N_f at $\sigma = 229$ MPa. These curves coincided well with each other. Crack was confirmed to initiate at $N \approx 1$ x 10^5 by a replica method.

The strain amplitude behaviour explained above is discussed on the basis of the appearance of slip bands. In the hydrogen-uncharged specimen, the rapid increase in the

FIGURE 5. *S-N* data for the hydrogen-charged and uncharged specimens of the 0.47% C steel without pre-fatigue.
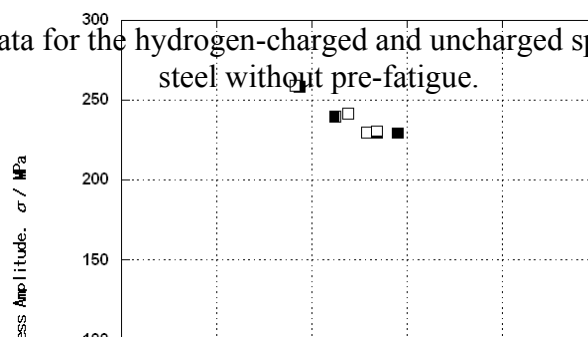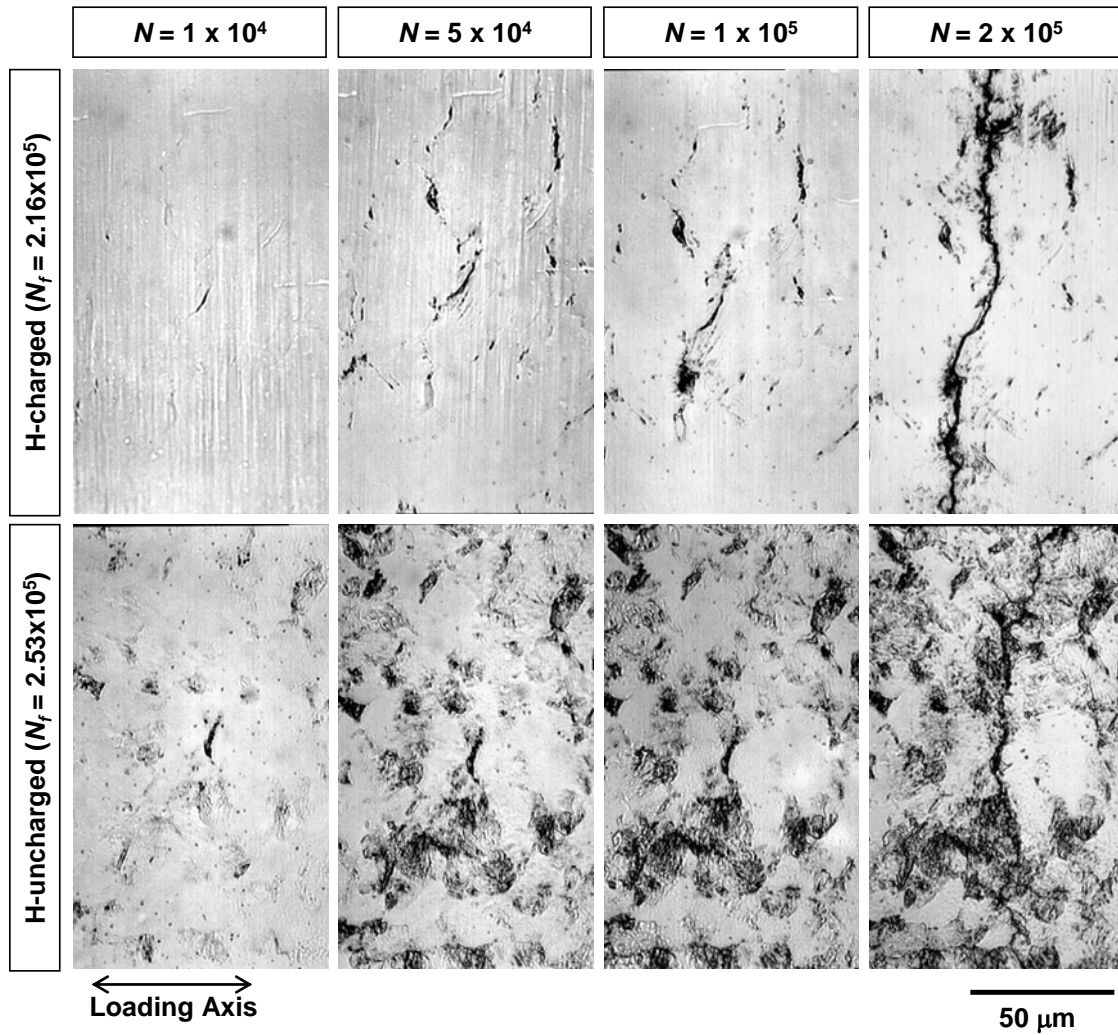
FIGURE 6. Slip bands and fatigue cracks of the hydrogen-charged and uncharged specimens of the 0.47% C steel. $\sigma = 230$ MPa, $K_t = 1.42$.
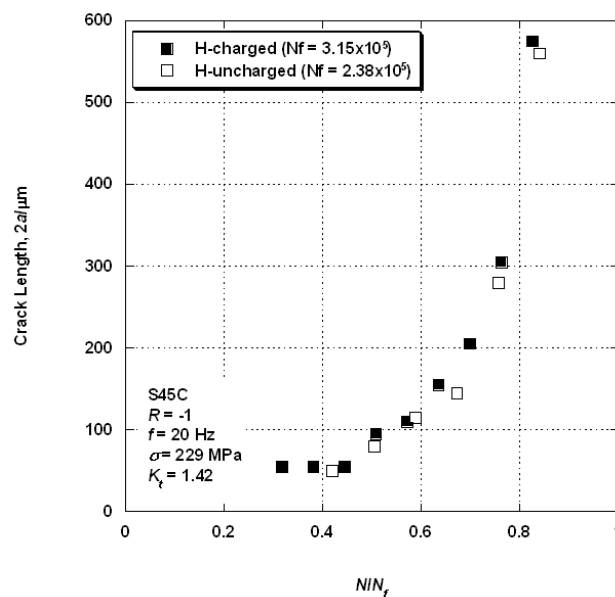

FIGURE 7. Crack growth curves of the hydrogen-charged and uncharged specimens of the 0.47% C steel.

strain amplitude, which corresponds to the yield point phenomenon, is due to the following: plastic deformation starts in a grain with the crystallographic orientation, in which slips are easy to act, and propagates every grain one after another. The amount of the strain shared by the individual slip bands in the hydrogen-charged specimen is less than that in the hydrogen-uncharged specimen. A decrease in the strain amplitude introduced by hydrogen charge is not caused by the dislocation locking mechanism, but is based on the localised slip bands.

Although the appearance of slip bands corresponds well to strain amplitude behaviour, the differences in fatigue life and crack initiation and propagation behaviour between the hydrogen-charged and uncharged specimens remain unclear. Further investigations are required on the effects of hydrogen charge at higher level.

Conclusion

In order to understand fundamental phenomena of metal fatigue in hydrogen environments of fuel cell (FC) systems, effects of hydrogen charge on cyclic stress-strain properties and fatigue behaviour in carbon steels were investigated. The conclusions can be summarised as follows.

(1) The hydrogen charge did not affect the stress-strain hysteresis loops in the 0.13% steel; on the other hand, the strain amplitude was decreased by hydrogen charge in the 0.47% C steel. This difference is due to the durability of the effect introduced by hydrogen charge, depending on hydrogen content and material.

(2) From the results of the constant stress amplitude tests of the 0.47% C steel, although the hydrogen-uncharged specimen presented a rapid increase in strain amplitude, which corresponded to yield point phenomenon, the strain amplitude of the hydrogen-charged specimen gradually increased. The saturation value of the hydrogen-charged specimen was lower than that of the hydrogen-uncharged specimen.

(3) The effect of hydrogen charge on the fatigue life was not remarkable, while a distinct difference in the appearance of the slip bands was observed between the hydrogen-charged and uncharged specimens. In the hydrogen-uncharged specimen slip bands widely distributed. In the hydrogen-charged specimen, the localised slip bands were observed. The decrease in the strain amplitude of the hysteresis loops introduced by hydrogen charge is caused by the localisation of slip bands. This behaviour may become noticeable if the hydrogen content is much higher. This is, therefore, the important phenomenon to be taken into consideration for studying the influence of hydrogen on metal fatigue.

References

1. Murakami, Y., *Metal Fatigue: Effects of Small Defects and Nonmetallic Inclusions*, Elsevier Ltd., Oxford, 2002.

2. Murakami, Y., Nomoto, T. and Ueda, T., *Fatigue Fract. Engng. Mater. Struct.*, vol. **22**, 581-590, 1999.

3. Murakami, Y., Yokoyama, N. N. and Nagata, J., *Fract. Engng. Mater. Struct.*, vol. **25**, 735-746, 2002.

4. Nagata, J. and Murakami, Y., *Proceedings of the 14th European Conference on Fracture*, 517-524, 2002.

5. Birnbaum, H. K. and Sofronis, P., *Mater. Sci. Eng. A*, Vol. **176**, 191-202, 1994.

6. Takaki, K. and Watanuki, R., *ISIJ Inter.*, Vol. **43**, 520-526, 2003.

7. Hagi, H. *Mater. Trans. JIM*, Vol. **35**, 168-173, 1994.